

# Adhesive Ion-Gel as Gate Insulator of Electrolyte-Gated Transistors

Jaehoon Jeong,<sup>[a, b]</sup> Surya Abhishek Singaraju,<sup>[a]</sup> Jasmin Aghassi-Hagmann,<sup>[a, c]</sup>  
Horst Hahn,<sup>[a, b, d]</sup> and Ben Breitung\*<sup>[a, e]</sup>

In this study, a facile method to fabricate a cohesive ion-gel based gate insulator for electrolyte-gated transistors is introduced. The adhesive and flexible ion-gel can be laminated easily on the semiconducting channel and electrode manually by hand. The ion-gel is synthesized by a straightforward technique without complex procedures and shows a remarkable ionic conductivity of  $4.8 \text{ mS cm}^{-1}$  at room temperature. When used as a gate insulator in electrolyte-gated transistors (EGTs), an on/off current ratio of  $2.24 \times 10^4$  and a subthreshold swing of  $117 \text{ mV dec}^{-1}$  can be achieved. This performance is roughly equivalent to that of ink drop-casted ion-gels in electrolyte-gated transistors, indicating that the film-attachment method might represent a valuable alternative to ink drop-casting for the fabrication of gate insulators.

Recently, electrolyte-gated transistors (EGTs) have attracted attention due to the rising interest in low-power, printed electronics, e.g., for radio-frequency identification (RFID) tags, displays, solar cells and Internet of Things applications. Further developments regarding EGTs were carried out, and many of them have focused on the gate insulator and the correlated

changes in EGT performance.<sup>[1–4]</sup> The gate insulator plays a pivotal role in the operation of EGTs since the current is switched on/off by an electric double layer (EDL) at the interface between the semiconductor and the gate insulator and/or channel. When a gate voltage is applied in an electrolytic gate insulator arrangement, the ions migrate to the interface, form EDLs and render the semiconducting channel conductive due to a field-effect. Since the conductivity of the channel is related to the formation of the EDLs, the ionic conductivity of the gating material is important to adjust the EGT regarding performance parameters like switching speed, drain current, on/off ratio, voltage sweep rates, etc.

However, comparably slow switching speeds, resulting from the necessity to form EDLs, remain a general drawback for EGTs. For decades, many types of gate insulators have been tested to improve the critical performance indicators of EGTs, among them, ABA triblock ion-gels are considered as cutting-edge gate insulators, as reported by Frisbie and Lodge.<sup>[1,5]</sup> Triblock ion-gels consist of triblock copolymers and ionic liquids. These triblock copolymers are tailorable, selectively soluble in ionic liquids and form physically cross-linked (PC) structures.<sup>[1,2,4,6,7]</sup> Dasgupta *et al.* reported on a composite solid polymer electrolyte (CSPE) for EGTs, where propylene carbonate is utilized as a plasticizer to increase the ion mobility inside the polymeric structures.<sup>[8]</sup>

In addition to conventional ion gel or polymer electrolyte-based gate insulators, various types of gate insulators have been developed using polymers or ionic liquids. For example, Ko *et al.* showed an ionic liquid-polymer gate insulator for flexible electronics.<sup>[9]</sup> Poly(4-vinylphenol) and [EMIM][TFSI] as ionic liquid are interacting by hydrogen bonds and form an ionic-polymer gate insulator.<sup>[9]</sup> It shows a high mechanical strength and thermal stability up to  $300^\circ\text{C}$  and exhibits stable gating performance in flexible zinc oxide (ZnO) thin-film transistors as gate insulator.<sup>[9]</sup> Moreover, Xu *et al.* reported polyacrylate copolymer gate insulators applied to organic field-effect transistors (OFETs).<sup>[10]</sup> This developed gate insulator, cured at  $230^\circ\text{C}$ , shows high dielectric strength and exhibited a remarkable gating performance, negligible hysteresis and on/off current ratio of  $10^5$  in OFETs.<sup>[10]</sup>

Besides the chemical structure of gate insulators, the fabrication technique is as well crucial in terms of printability and can severely affect the performance of printed EGTs. Conventional techniques, like ink-jet printing or aerosol-jet printing, are known for the fabrication of high-performance EGTs, mostly due to their high printing accuracy. Nevertheless, the utilized inks for these procedures have to be adjusted


[a] J. Jeong, S. A. Singaraju, Prof. Dr. J. Aghassi-Hagmann, Prof. Dr. H. Hahn, Dr. B. Breitung  
Institute of Nanotechnology (INT),  
Karlsruhe Institute of Technology (KIT)  
Eggenstein-Leopoldshafen, 76344, Germany  
E-mail: ben.breitung@kit.edu


[b] J. Jeong, Prof. Dr. H. Hahn  
Joint Research Laboratory Nanomaterials – Technische Universität Darmstadt  
and Karlsruhe Institute of Technology (KIT)  
Otto-Berndt-Str. 3, 64206 Darmstadt, Germany

[c] Prof. Dr. J. Aghassi-Hagmann  
Department of Electrical Engineering and Information Technology,  
Offenburg University of Applied Sciences  
Offenburg 77652, Germany

[d] Prof. Dr. H. Hahn  
Helmholtz Institute Ulm for Electrochemical Energy Storage  
Helmholtzstr. 11, 89081 Ulm, Germany

[e] Dr. B. Breitung  
Karlsruhe Nano Micro Facility,  
Karlsruhe Institute of Technology  
Eggenstein-Leopoldshafen, 76344, Germany

 Supporting information for this article is available on the WWW under <https://doi.org/10.1002/celec.202000305>

 © 2020 The Authors. Published by Wiley-VCH Verlag GmbH & Co. KGaA. This is an open access article under the terms of the Creative Commons Attribution Non-Commercial License, which permits use, distribution and reproduction in any medium, provided the original work is properly cited and is not used for commercial purposes.

regarding viscosity, drying behavior, and other fluidic properties. An example for aerosol-jet printable gate insulators of EGTs is the already-mentioned ABA triblock ion-gels.<sup>[11,11]</sup> Additionally, Marques *et al.* reported about ink-jet printing of CSPE as gate insulator for n-type  $\text{In}_2\text{O}_3$ -based EGTs.<sup>[12]</sup> Despite the advantages of aerosol and ink-jet printing, other methods to prepare gate insulators on EGTs are under investigation as well. Lee *et al.* suggested a fabrication technique of a gate insulator using a rubbery ion-gel, which can be cut by hand and laminated on electric circuits and EGTs.<sup>[3]</sup>

In this study, we introduce an adhesive ion-gel (AIG) as a gate insulator, synthesized with a facile fabrication method. The AIG can be easily cut to the desired shapes and laminated on substrates or electrodes due to adhesive and flexible material characteristics. Additionally, the AIG can be drawn off and used again without severe losses of the ionic conductivity and does, therefore, not impede transistor performances. The AIG can easily adhere to diverse substrates such as wood, glass, plastic, and metal (Figure S1).

The AIG was prepared using poly(vinyl alcohol) (PVA), poly(methyl vinyl ether-*alt*-maleic anhydride) (PMVE-MA), dimethyl sulfoxide (DMSO) and 1-ethyl-3-methylimidazolium triflate ([EMIM][OTf]). PVA and PMVE-MA constitute the backbone polymer and the chemical cross-linker, while [EMIM][OTf] and DMSO represent the ion source and the solvent, respectively.

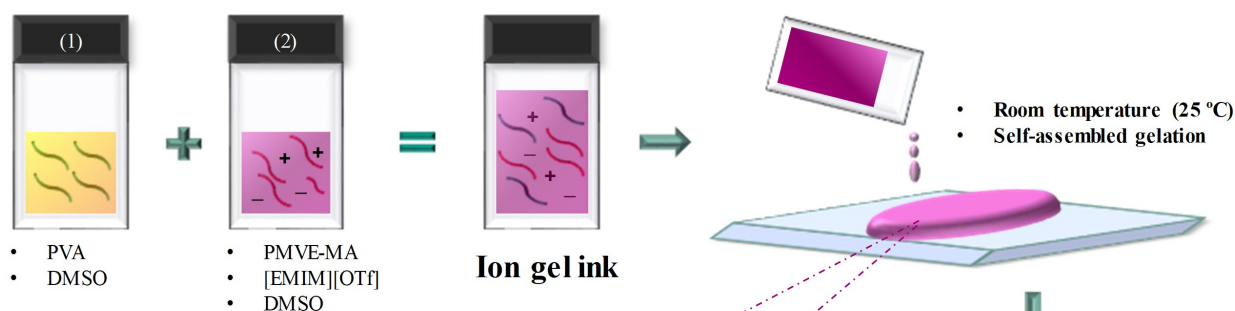
Among the ingredients, the functional groups of methyl vinyl ether (MVE) and carboxylic acid of PMVE-MA lead to the adhesive characteristic of the AIG. MVE is known as an integral part of pressure-sensitive adhesives, and can form elastomeric

adhesive surfaces.<sup>[13,14]</sup> In addition, the carboxylic acid groups, cleaved from maleic anhydride, can improve the adhesion by forming hydrogen bonds. This possibility to form hydrogen bonds has already led to the unitization of PMVE-MA in bioadhesives.<sup>[15–17]</sup>

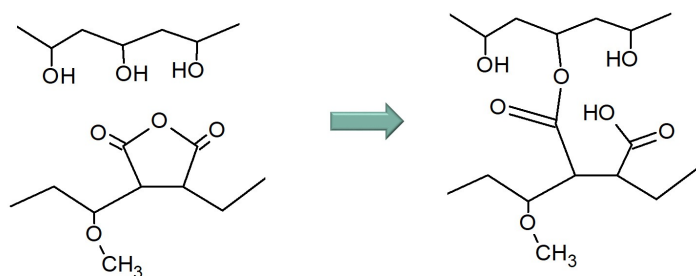
The AIG is synthesized by blending two polymer solutions, which contain the above-mentioned ingredients. As shown in Scheme 1, solution (1) contains PVA dissolved in DMSO, and solution (2) contains a mixture of PMVE-MA and [EMIM][OTf] dissolved in DMSO, respectively. During mixing, the hydroxyl group of PVA and the cyclic anhydride of PMVE-MA spontaneously react and form a chemically cross-linked (CC) gel structure by ring-opening esterification.<sup>[18]</sup> The cross-linking rate depends on the AIG ingredient ratio. Using an optimized ratio, the gelation deriving from cross-linking is completed within a few hours. To ensure that all maleic anhydrides can react with the respective hydroxyl groups, the AIG is aged overnight before utilization. This synthesis process does not require a subsequent treatment, e.g. UV-curing,<sup>[19,20]</sup> to form a functional AIG. The CC structures could be identified by Fourier-transform infrared (FT-IR) spectroscopy (Figure 1).

In the spectrum of PMVE-MA (Figure 1b), peaks at  $1856\text{ cm}^{-1}$  and  $1783\text{ cm}^{-1}$  are attributed to the  $\text{C}=\text{O}$  symmetric/asymmetric stretching bands of maleic anhydride.<sup>[21]</sup> These two peaks disappear in the spectrum of the blended PVA/PMVE-MA gel (Figure 1c), and overlapping  $\text{C}=\text{O}$  peaks of carboxylic acid ( $1718\text{ cm}^{-1}$ ) and ester ( $1720\text{ cm}^{-1}$ ) are observed.<sup>[22–24]</sup> These changes result from cleavage of the cyclic anhydride (PMVE-MA) by the hydroxyl groups of PVA over ring-opening

### (a) Synthesis of adhesive ion gel



### (b) Ring-opening esterification



### (c) Adhesive ion gel

**Scheme 1.** Schematic illustration of the adhesive ion-gel; a) the ink preparation for synthesis, b) the ring-opening esterification, and c) the adhesive ion-gel.

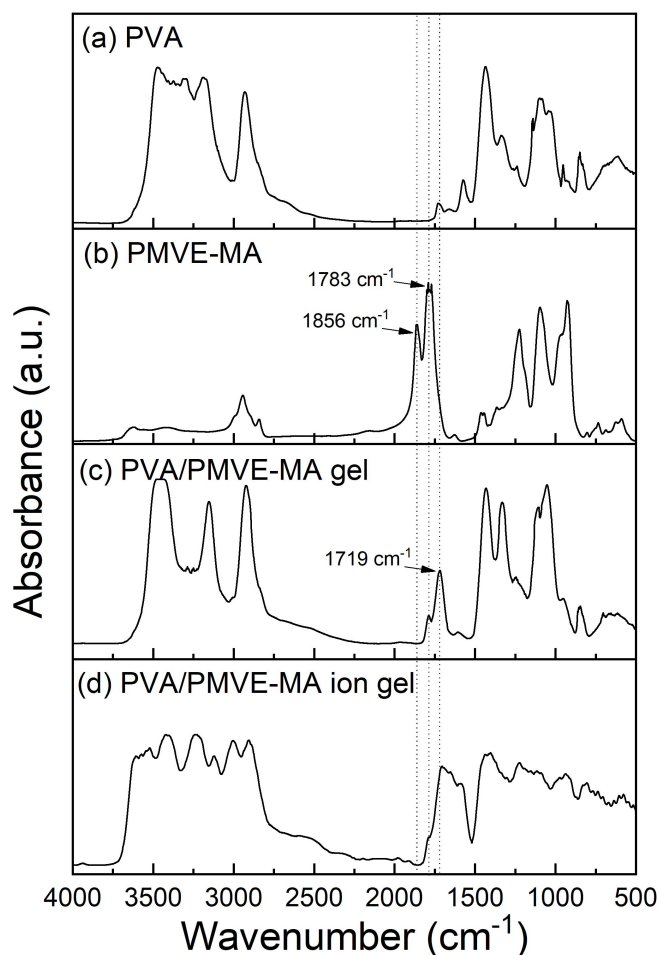


**Figure 1.** Absorbance spectra of Fourier-transform infrared spectroscopy (FT-IR); a) PVA film, b) PMVE-MA pellet with KBr, c) PVA/PMVE-MA gel film, and d) PVA/PMVE-MA ion-gel (adhesive ion-gel) film. PMVE-MA is pelletized by hydraulic pressure because of the difficulty to make a polymer film. DMSO is fully evaporated for film making of PVA, PVA/PMVE-MA gel, and PVA/PMVE-MA ion-gel.

esterification, which transforms the compound into a carboxylic acid and an ester (Scheme 1b). During the process, [EMIM][OTf] is captured into the CC gel structures. Following this procedure, the AIG can easily be synthesized without complex techniques (Scheme 1c).

To investigate the electric properties of the AIG, frequency-dependent behavior and ionic conductivity are analyzed by electrochemical impedance spectroscopy (EIS). Bulk films of the AIG are assembled and measured in a Swagelok cell setup (Figure 2a). In Figure 2b, the Bode plot shows a plateau region of  $\log(|Z|)$  indicating bulk resistance ( $R_{\text{bulk}}$ ) in the high-frequency range ( $> 30$  kHz). In this frequency range, the conducting ions of [EMIM] and [OTf] cannot migrate fast enough into the gel matrix to form the EDLs due to the high frequencies.<sup>[25]</sup> However, in the lower frequency range ( $< 9.3$  kHz), where the phase angle is lower than  $-45^\circ$ , [EMIM] and [OTf] can migrate into the gel matrix and form the EDLs, indicating capacitive behavior.<sup>[1,26]</sup> Below 1 kHz, a phase angle of around  $70^\circ$  is observed (ideal capacitive behavior at a phase

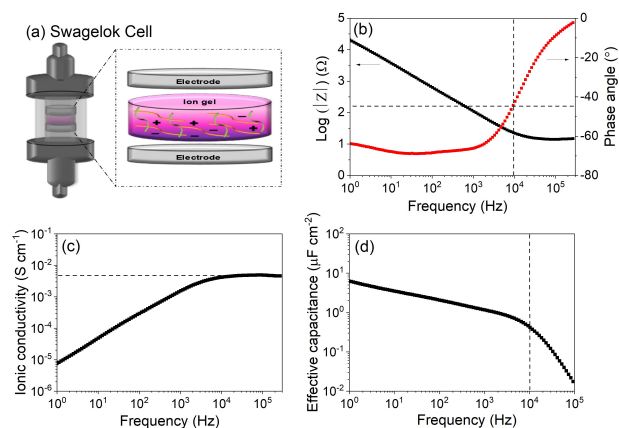


**Figure 2.** The plots of electrochemical impedance spectroscopy of PVA/PMVE-MA ion-gel; a) illustration of Swagelok cell and adhesive ion-gel, b) Bode plot, c) ionic conductivity versus frequency plot, and d) specific capacitance versus frequency plot. Film thickness and diameter are 0.76 mm and 12 mm.

angle of  $-90^\circ$ ), and the value of  $\log(|Z|)$  is linearly increased by the influence of the EDL formation when the frequency is decreased.

The ionic conductivity ( $\sigma$ ), which is a crucial property and affecting the gating performance in EGTs, can be calculated with the results of the impedance spectroscopy using Equation (1).

$$\sigma = \frac{d}{AZ_{re}} \quad (1)$$

$A$  is the surface area,  $d$  is the thickness of the AIG, and  $Z_{re}$  is the real part of the measured impedance. In Figure 2c, the ionic conductivity in the frequency region ( $> 30$  kHz), where only resistance from ion migration is measured without the influence of dipole relaxation or EDLs, is calculated to  $4.8 \text{ mS cm}^{-1}$ .<sup>[1,26]</sup> Below 9.3 kHz, the ionic conductivity linearly decreases with decreasing frequency, because the electrode polarization, caused by the EDLs, hinders the ion mobility.<sup>[27,28]</sup>

Additionally, the capacitance is measured to determine the gating performance because the capacitance is proportional to the drain-source current through the semiconducting channel during transistor operation. The capacitance, stemming from the EDLs between AIG and electrode/channel surface, can be measured as an effective capacitance ( $C_{\text{eff}}$ ) in EIS measurements. The  $C_{\text{eff}}$  calculated by Equation (2), varies with the applied frequency and can be calculated based on the frequency-dependent behavior of the AIG as shown in Figure 2b.

$$C_{\text{eff}} = \frac{-Z_{\text{im}}}{2\pi f A |Z|^2} \quad (2)$$

$Z_{\text{im}}$  is the imaginary part of the measured impedance,  $f$  is the frequency, and  $A$  is the surface area between the electrode and the ion-gel film. Figure 2d shows the two different frequency regions, classified to high- and low-frequency. In the high-frequency region ( $> 9.3$  kHz), the  $C_{\text{eff}}$  drastically drops due

to insufficient time for EDL formation at the interface of the electrodes. On the other hand, below 0.3 kHz, conducting ions can migrate to form EDLs, and the  $C_{\text{eff}}$  linearly increases according to the decreased frequency. The  $C_{\text{eff}}$  value is calculated to  $6.23 \mu\text{F cm}^{-2}$  at 1 Hz. These results confirm that the AIG shows typical frequency-dependent behavior (e.g., like gel polymer electrolytes) and demonstrates remarkable ionic conductivity and effective capacitance. These parameters are closely related to the transistor performance. Therefore, it follows that optimization as studied in<sup>[29]</sup> of the ionic mobility/resistance and material/device parameters of the EGTs should be carried out to achieve the highest possible cutoff frequencies on transistor level.

To analyze the gating performance of the AIG, EGTs were fabricated as shown in Figure 3a. Gate, drain and source electrodes were patterned on an indium tin oxide (ITO)-deposited glass substrate using laser ablation. An  $\text{In}_2\text{O}_3$  precursor ink was ink-jet printed between source and drain electrodes and annealed to  $400^\circ\text{C}$  for 2 h. After the annealing process, n-type semiconducting channels of indium oxide ( $\text{In}_2\text{O}_3$ ) were prepared.<sup>[30]</sup> The AIG film was laminated on an in-plane structure of the semiconducting channel and electrodes by hand. As shown in Figure 3a, the AIG can be adhesively attached to the in-plane EGT on a glass substrate without any temperature/chemical post-treatment.

In drain-source current ( $I_d$ ) versus gate-source voltage ( $V_g$ ) plots (Figure 3b), the AIG-gated EGTs show remarkable gating performances. The transfer curves of the EGTs show narrow hysteresis, indicating that the formation and deformation of EDLs are fast enough due to the high ionic conductivity of the AIG. Even though the adhesive ion-gel is laminated by hand, it remains tightly attached on the electrodes and the semiconducting channel, and exhibits stable transfer curves. The threshold voltage ( $V_{\text{th}}$ ) is calculated to  $-0.36 \text{ V}$  by the extrapolation of  $I_d^{1/2}$ . The on/off current ratio ( $I_{\text{on}}/I_{\text{off}}$ ) and the subthreshold swing (SS) are calculated to  $2.24 \times 10^4$  and

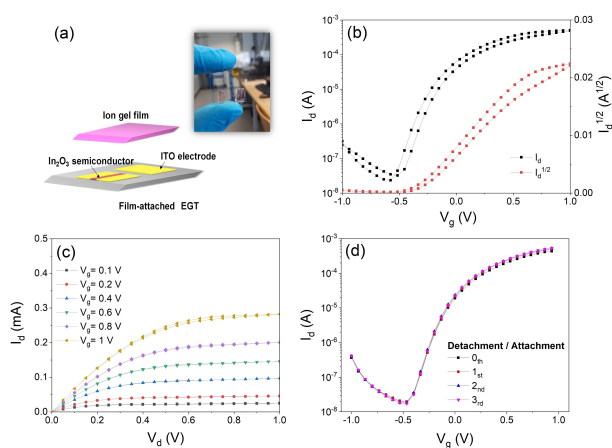


**Figure 3.** Characterization of in-plane, film-attached EGTs; a) illustration and picture of in-plane, film-attached EGTs, b) transfer curves in gate-source voltage ( $V_g$ ) versus drain-source current ( $I_d$ ) and  $I_d^{1/2}$  plots at 1 V of drain-source voltage ( $V_d$ ), c) output characteristic curves in  $V_d$  versus  $I_d$  plot at different  $V_g$ , and d)  $V_g$  versus  $I_d$  plots for attachment/detachment test of ion-gel film. Channel width and length are 2 mm and 50  $\mu\text{m}$ .

117.24  $\text{mV dec}^{-1}$ , respectively. Additionally, the AIG could be removed and reattached to the surface several times, without a considerable loss of gating performances. Figure 3d shows stable transfer curves of an EGT, indicating an electric performance independent of the times the AIG was re/attached. Therefore, it identifies the reusability of the AIG films in the EGTs.

Lastly, two types of AIG-gated EGTs, using different fabrication techniques are compared to investigate the impact of the fabrication technique on EGT performance. Figure 4 shows the output curves of EGTs where the AIG is applied as gating material by manually attaching and ink drop-casting using a pipette, respectively. The recipe of the AIG is not changed in both cases. In the fabrication of EGTs by ink drop-casting, the ink was deposited directly on the semiconducting channel and electrodes before the gelation. Then, the dropped inks were gelated and became adhesive ion-gels for use as gate insulators (Figure S2). Figure 4 shows the transfer curves of both EGT types, where the EGTs show an almost similar performance. The detailed values for  $I_{\text{on}}/I_{\text{off}}$ , SS and  $V_{\text{th}}$  can be found in Table S1. This result shows that the surficial contact by film-attachment is equivalent to that by ink drop-casting, so both EGTs exhibit similar EGT performance.

In conclusion, an adhesive and flexible ion-gel has been developed and used as gate insulators for EGTs. The adhesion of the AIG allows fabricating gate insulators even manually. The film-attachment method of the AIG does not need to consider adverse effects of solvents, such as swelling, dissolution, and penetration of polymer or organic components during the fabrication of multi-layer structures during printing.<sup>[31,32]</sup> The AIG shows remarkable ionic conductivity and effective capacitance and can be simply stripped away and reattached to the EGT without performance losses. This reusability of the AIG is advantageous for low-cost electronics in terms of saving materials.<sup>[33,34]</sup> The film-attached EGTs show the performance comparable to ink drop-casted EGTs. These results show that it is possible to synthesize ionic-conductive “stickers” and that

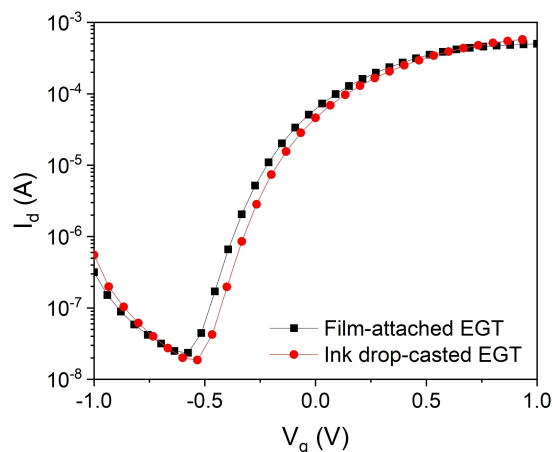


**Figure 4.**  $V_g$  versus  $I_d$  plots of ion-gel film-attached EGT (black) and ink drop-casted EGT (red). Channel width and length are 2 mm and 50  $\mu\text{m}$ . Humidity level and temperature are room conditions.



easy utilization in EGTs is possible without any performance deterioration.

## Acknowledgements

J.J. acknowledges the German Academic Exchange Service (DAAD, Ref. no. 91650506). H.H. and J.A.–H acknowledge the funding received from Helmholtz Association under the Virtual Institute VI-530 “Printed electronics based on inorganic nanomaterials: From atoms to functional devices and circuits”. S.A.S. acknowledge the Ministry of Science, Research and Arts of the state of Baden Württemberg for funding research through the MERAGEM graduate school. B.B. and H.H. appreciate the support of EnABLES, a project funded by the European Union’s Horizon 2020 research and innovation program under grant agreement no. 730957.

## Conflict of Interest

The authors declare no conflict of interest.

**Keywords:** adhesive ion gels · electrolyte-gated transistors · ionic liquids · ion gels · printed electronics

- [1] J.-H. Choi, W. Xie, Y. Gu, C. D. Frisbie, T. P. Lodge, *ACS Appl. Mater. Interfaces* **2015**, *7*, 7294–7302.
- [2] J. Lee, M. J. Panzer, Y. He, T. P. Lodge, C. D. Frisbie, *J. Am. Chem. Soc.* **2007**, *129*, 4532–4533.
- [3] K. H. Lee, M. S. Kang, S. Zhang, Y. Gu, T. P. Lodge, C. D. Frisbie, *Adv. Mater.* **2012**, *24*, 4457–4462.
- [4] Y. Choi, J. Kang, E. B. Secor, J. Sun, H. Kim, J. A. Lim, M. S. Kang, M. C. Hersam, J. H. Cho, *Adv. Funct. Mater.* **2018**, *28*, 1802610.
- [5] J. H. Cho, J. Lee, Y. Xia, B. Kim, Y. He, M. J. Renn, T. P. Lodge, C. D. Frisbie, *Nat. Mater.* **2008**, *7*, 900–906.
- [6] Y. He, P. G. Boswell, P. Bühlmann, T. P. Lodge, *J. Phys. Chem. B* **2007**, *111*, 4645–4652.
- [7] Y. Gu, S. Zhang, L. Martinetti, K. H. Lee, L. D. McIntosh, C. D. Frisbie, T. P. Lodge, *J. Am. Chem. Soc.* **2013**, *135*, 9652–9655.
- [8] S. Dasgupta, G. Stoesser, N. Schweikert, R. Hahn, S. Dehm, R. Kruk, H. Hahn, *Adv. Funct. Mater.* **2012**, *22*, 4909–4919.
- [9] J. Ko, S. J. Lee, K. Kim, E. Lee, K.-H. Lim, J.-M. Myoung, J. Yoo, Y. S. Kim, *J. Mater. Chem. C* **2015**, *3*, 4239–4243.
- [10] W. Xu, S.-W. Rhee, *Org. Electron.* **2010**, *11*, 836–845.
- [11] J. H. Cho, J. Lee, Y. Xia, B. Kim, Y. He, M. J. Renn, T. P. Lodge, C. D. Frisbie, *Nat. Mater.* **2008**, *7*, 900–906.
- [12] G. Cadilha Marques, F. von Seggern, S. Dehm, B. Breitung, H. Hahn, S. Dasgupta, M. B. Tahoori, J. Aghassi-Hagmann, *IEEE Trans. Electron Devices* **2019**, *66*, 2202–2207.
- [13] C. E. Schildknecht, A. O. Zoss, C. McKinley, *Ind. Eng. Chem.* **1947**, *39*, 180–186.
- [14] D. F. Moore, W. Geyer, *Wear* **1972**, *22*, 113–141.
- [15] P. A. McCarron, A. D. Woolfson, R. F. Donnelly, G. P. Andrews, A. Zawislak, J. H. Price, *J. Appl. Polym. Sci.* **2004**, *91*, 1576–1589.
- [16] K. Yoncheva, E. Lizarraga, J. M. Irache, *Eur. J. Pharm. Sci.* **2005**, *24*, 411–419.
- [17] P. Arbós, M. A. Arangoa, M. A. Campanero, J. M. Irache, *Int. J. Pharm.* **2002**, *242*, 129–136.
- [18] J. Jeong, G. C. Marques, X. Feng, D. Boll, S. A. Singaraju, J. Aghassi-Hagmann, H. Hahn, B. Breitung, *Adv. Mater. Interfaces* **2019**, *6*, 1901074.
- [19] G. Martínez-Ponce, C. Solano, *Opt. Express* **2006**, *14*, 3776.
- [20] J.-H. Choi, Y. Gu, K. Hong, W. Xie, C. D. Frisbie, T. P. Lodge, *ACS Appl. Mater. Interfaces* **2014**, *6*, 19275–19281.
- [21] B. Schneider, O.-D. Hennemann, W. Possart, *J. Adhes.* **2002**, *78*, 779–797.
- [22] W.-Y. Chiang, C.-M. Hu, *J. Appl. Polym. Sci.* **1985**, *30*, 3895–3910.
- [23] C. Rohatgi, N. Dutta, N. Choudhury, *Nanomaterials* **2015**, *5*, 398–414.
- [24] E. Peng, E. S. G. Choo, C. S. H. Tan, X. Tang, Y. Sheng, J. Xue, *Nanoscale* **2013**, *5*, 5994–6005.
- [25] J. Kang, J. Wen, S. H. Jayaram, A. Yu, X. Wang, *Electrochim. Acta* **2014**, *115*, 587–598.
- [26] O. Larsson, E. Said, M. Berggren, X. Crispin, *Adv. Funct. Mater.* **2009**, *19*, 3334–3341.
- [27] N. Shukla, A. K. Thakur, A. Shukla, D. T. Marx, *Int. J. Electrochem. Sci.* **2014**, *9*, 16.
- [28] Z. Osman, M. I. Mohd Ghazali, L. Othman, K. B. Md Isa, *Results Phys.* **2012**, *2*, 1–4.
- [29] X. Feng, C. Punckt, G. C. Marques, M. Hefenbrock, M. B. Tahoori, J. Aghassi-Hagmann, *IEEE Trans. Electron Devices* **2019**, *66*, 3365–3370.
- [30] S. K. Garlapati, N. Mishra, S. Dehm, R. Hahn, R. Kruk, H. Hahn, S. Dasgupta, *ACS Appl. Mater. Interfaces* **2013**, *5*, 11498–11502.
- [31] L. Zhang, C. Di, Y. Zhao, Y. Guo, X. Sun, Y. Wen, W. Zhou, X. Zhan, G. Yu, Y. Liu, *Adv. Mater.* **2010**, *22*, 3537–3541.
- [32] K.-J. Baeg, *ETRI J* **2011**, *33*, 887–896.
- [33] C. Qian, J. Sun, J. Yang, Y. Gao, *RSC Adv.* **2015**, *5*, 14567–14574.
- [34] I. Cunha, R. Barras, P. Grey, D. Gaspar, E. Fortunato, R. Martins, L. Pereira, *Adv. Funct. Mater.* **2017**, *27*, 1606755.

Manuscript received: February 25, 2020  
Revised manuscript received: April 14, 2020  
Accepted manuscript online: April 15, 2020